International Journal of Pharmaceutics 421 (2011) 160–169

Contents lists available at SciVerse ScienceDirect

International Journal of Pharmaceutics

journal homepage: www.elsevier.com/locate/ijpharm

Pharmaceutical Nanotechnology

Dual targeting folate-conjugated hyaluronic acid polymeric micelles for paclitaxel delivery

Yanhua Liu[a], Jin Sun[a,*], Wen Cao[a], Jianhong Yang[b], He Lian[a], Xin Li[a], Yinghua Sun[a], Yongjun Wang[a], Siling Wang[a], Zhonggui He[a,*]

[a] Department of Biopharmaceutics, School of Pharmacy, Shenyang Pharmaceutical University, China
[b] Department of Pharmaceutics, School of Pharmacy, Ningxia Medical University, 750004, China

ARTICLE INFO

Article history:
Received 20 July 2011
Received in revised form 4 September 2011
Accepted 11 September 2011
Available online 16 September 2011

Keywords:
Hyaluronic acid
Hyaluronic acid-octadecyl
Folate-hyaluronic acid-octadecyl
Polymeric micelles
Paclitaxel

ABSTRACT

A series of novel self-assembled hyaluronic acid derivatives (HA-C_{18}) grafted with hydrophobic octadecyl moiety and further dual targeting folic acid-conjugated HA-C_{18} (FA-HA-C_{18}) were synthesized. With the increase in the degree of substitution of octadecyl group from 12.7% to 19.3%, the critical micellar concentration of HA-C_{18} copolymers decreased from 37.3 to 10.0 μg/mL. Paclitaxel (PTX) was successfully encapsulated into the hydrophobic cores of the HA-C_{18} and FA-HA-C_{18} micelles, with encapsulation efficiency as high as 97.3%. The physicochemical properties of the polymeric micelles were measured by DLS, TEM and DSC. Moreover, in vitro release behavior of PTX was investigated by dialysis bag method and PTX was released from micelles in a near zero-order sustained manner. In vitro antitumor activity tests suggested PTX-loaded HA-C_{18} and FA-HA-C_{18} micelles exhibited significantly higher cytotoxic activity against MCF-7 and A549 cells compared to Taxol at a lower PTX concentration. The cellular uptake experiments were conducted by quantitative assay of PTX cellular accumulation and confocal laser scanning microscopy imaging of coumarin-6 labeled HA-C_{18} and FA-HA-C_{18} micelles in folate receptor overexpressing MCF-7 cells. Folate and CD44 receptor competitive inhibition studies performed by fluorescence microscopy imaging suggested intracellular delivery of HA-C_{18} and FA-HA-C_{18} micelles were efficiently taken up via CD44 receptor-mediated endocytosis. The folate receptor-mediated endocytosis further enhanced internalized amounts of FA-HA-C_{18} micelles in MCF-7 cells, as compared with HA-C_{18} micelles. The internalization pathways of PTX-loaded HA-C_{18} and FA-HA-C_{18} micelles might include clathrin-mediated endocytosis, caveolae-mediated endocytosis and macropinocytosis. Therefore, the present study suggested that HA-C_{18} and FA-HA-C_{18} copolymers as biodegradable, biocompatible and cell-specific targetable nanostructure carriers, are promising nanosystems for cellular and intracellular targeting delivery of hydrophobic anticancer drugs.

1. Introduction

Paclitaxel (PTX) has been extensively used for treatment of various types of cancers in clinic. The conventional commercial formulation, Taxol, contains a 50:50 (v/v) mixture of Cremophor EL and absolute ethanol for enhancing the solubility of PTX in water. However, severe side effects of Cremophor EL, such as hypersensitivity, neurotoxicity and neuropathy, have limited its use in cancer therapy (Lee et al., 2008). To minimize its side effects, various drug delivery systems, including liposomes (Crosasso et al., 2000), cyclodextrin complexes (Sharma et al., 1995), emulsions (Kan et al., 2005), nanospheres (Fonseca et al., 2002), polymer conjugates (Dosio et al., 2010) and polymeric micelles (Wang et al., 2008; Zhang et al., 2008) have been developed. Among these studied approaches, the polymeric micellar system is considered as one of the most promising approaches because of high drug loading, sustained release, enhanced cellular uptake and tumor targeting.

Polymeric micelle self-assembly by amphiphilic graft copolymers in aqueous solution has received growing scientific attention over the years (Jones and Leroux, 1999). Among the polymeric micelles, hydrophobized polysaccharides have currently become one of the hottest research areas in the field of drug delivery nanosystems. Self-assembled hydrophobized polysaccharide polymeric micelles are widely employed as promising carriers of water-insoluble drugs, and show high solubilization capacity and stability, sustained release, prolonged circulation, and tumor localization by enhanced permeability and retention (EPR) effect

* Corresponding authors at: Mailbox 59#, School of Pharmacy, Shenyang Pharmaceutical University, No. 103 Wenhua Road, Shenyang 110016, China. Tel.: +86 24 23986321; fax: +86 24 23986321.
E-mail addresses: sunjin66@21cn.com (J. Sun), hezhonggui@gmail.com, Hezhgui_student@yahoo.com (Z. He).

0378-5173/$ – see front matter Crown Copyright © 2011 Published by Elsevier B.V. All rights reserved.
doi:10.1016/j.ijpharm.2011.09.006

(Akiyoshi et al., 1993; Torchilin, 2001; Akiyoshi and Sunamoto, 1996).

Hyaluronic acid (HA) has been found increasing biotechnological and biomedical applications (Grigorij et al., 2007). HA has several advantages for the pharmaceutical application, including wide variety of sources, biocompatibility, biodegradability, non-toxicity, non-immunogenicity and abundance of functional groups (–COOH, –OH) for modification or functionalization (Choi et al., 2009, 2010). In particular, HA is an important signal for activating kinase pathways and regulating angiogenesis in tumor. It has a strong affinity with cell-specific surface markers such as glycoprotein CD44 and receptor for HA-mediated motility (RHAMM), which are abundantly overexpressed on the surface of many types of tumors. Thus, tumor cells exhibit enhanced binding and uptake of HA, and then HA and its derivatives have been widely used as ligands for tumor targeted drug delivery (Jaracz et al., 2005; Larsen and Balazs, 1991). In recent years, hydrophobized HA derivatives, such as PLGA grafted HA loading with doxorubicin (Lee et al., 2009), 5β-cholanic acid-HA (Choi et al., 2009, 2010), HA-PTX (Lee et al., 2008), and HA-amino acid-PTX (Xin et al., 2010), have generated significant attention in the area of polymeric micelles due to their enhanced targeting ability to the tumor and higher therapeutic efficacy.

Dual receptors targeting, a novel strategy for targeted drug delivery, can effectively and specifically target nanoparticles to tumor cells. Recently, this approach has been utilized in the field of drug delivery nanosystem (Ying et al., 2010; Saul et al., 2006). In our study, HA polymer was selected as polysaccharide main chain for hydrophobized modification due to its specific targeting to tumor cells via CD44 receptor. The further conjugating folic acid to HA-C_{18} copolymer could achieve the dual active targeting. That is, we developed a self-assembled HA-octadecyl (HA-C_{18}) copolymer by chemical conjugation of hydrophobic octadecyl group and further to synthesis folate-conjugated HA-octadecyl (FA-HA-C_{18}) copolymer for active dual targeting. Then PTX was successfully encapsulated by HA-C_{18} and FA-HA-C_{18} polymeric micelles. The physicochemical characterization, in vitro cytotoxicity and cellular uptake of the developed polymeric micelles were studied in detail.

2. Materials and methods

2.1. Materials

Sodium hyaluronate (MW = 11 kDa) was purchased from Shandong Freda Biopharm Co. Ltd. (Shandong, China). Octadecylamine was purchased from Guangzhou Jingwei Pharm Co. Ltd. (Guangzhou, China). Folic acid was obtained from Wuhan Yuancheng Technology Development Co. Ltd. (Wuhan, China). PTX was purchased from Chongqing Meilian Pharm Co. Ltd. (Chongqing, China). 1-Ethyl-3-(3-dimethylaminopropyl) carbodiimide (EDC) was obtained from Zhejiang Pukang Pharm Co. Ltd. (Zhejiang, China). N-hydroxysuccinimide (NHS) and dicyclohexylcarbodiimide (DCC) were purchased from Shanghai Medpep Co. Ltd. (Shanghai, China). Pyrene, coumarin-6, 3-(4,5-dimethylthiazol-2-yl)-2,5-diphenyl-tetrazolium bromide (MTT), propidium iodide (PI) and trypsin were supplied by Sigma–Aldrich Co. (St. Louis, MO, USA). Dulbecco's modified Eagle's medium (DMEM) and RPMI-1640 were purchased from Gibco (BRL, MD, USA). Polyethylene glycol 400 (PEG 400), formamide, N,N-dimethylformamide (DMF) and dimethyl sulfoxide (DMSO) were supplied by Shandong Yuwang Chemical Reagent Co. Ltd. (Shandong, China). All other reagents were of analytical or chromatographic grade.

2.2. Synthesis of HA-C_{18} conjugate

HA (100 mg, 2.5×10^{-4} mol, number of moles of –COOH) was dissolved in anhydrous formamide (5 mL) by gentle heating. After the solution was cooled to room temperature, two molar excess of EDC (96 mg) and NHS (58 mg) were added and stirred for 2 h to activate the carboxylic group of sodium hyaluronate. Then various amounts of octadecylamine (the mole ratio of octadecylamine to –COOH of HA was varied as 1/2, 1/1, 3/2) dissolved in anhydrous DMF were added slowly to the HA solution, and the reaction mixture was stirred at 60 °C under a nitrogen atmosphere for 5 h. The mixture was stirred for further 24 h at room temperature. The resultant mixture dialyzed against excess amount of water/ethanol (1 v/3 v–1 v/1 v) for 2 days and distilled water for 2 days, respectively. Finally, the solution was filtered to remove other impurities, followed by lyophilization (Choi et al., 2009; Park et al., 2006). The octadecylamine content in the conjugate was determined using ^{1}H NMR in DMSO-d_6.

2.3. Synthesis of FA-HA-C_{18} conjugate

To synthesis FA-HA-C_{18} conjugate, folic acid (220 mg) dissolved in anhydrous DMSO (10 mL) was reacted with DCC (1030 mg) and NHS (288 mg) at 21 °C for 5 h in the dark. After the reaction completed, a white precipitate was filtered and the filtrate was added slowly to the HA-C_{18} conjugate (the degree of substitution (DS) of octadecyl was 19.3%) dissolved in anhydrous formamide (10 mL). The reaction mixture was reacted at room temperature for 48 h in the dark. After the reaction, the resultant solution was first dialyzed against excess amount of $NaHCO_3$–Na_2CO_3 buffer solution (pH 10) until no folic acid could be detected in the dialysate by measuring UV absorbance at 281 nm, and subsequently dialyzed against distilled water for 3 days. Finally, the dialyzed solution was lyophilized (Zheng et al., 2009; Wang et al., 2010). DS of folic acid in FA-HA-C_{18} was calculated by UV absorbance at 360 nm using folic acid unmodified HA-C_{18} as reference.

2.4. Characteristics of HA-C_{18} and FA-HA-C_{18} conjugates

2.4.1. Nuclear magnetic resonance spectroscopy (NMR)

^{1}H NMR spectra of HA, HA-C_{18} and FA-HA-C_{18} were analyzed on a NMR Spectrometer (300 Hz, Bruker, Switzerland). HA was dissolved in D_2O, and HA-C_{18}, FA-HA-C_{18} were dissolved in DMSO-d_6, respectively.

2.4.2. Measurement of critical micellar concentration (CMC)

To quantitatively validate the core–shell forming property, the CMC of HA-C_{18} and FA-HA-C_{18} conjugates was measured by fluorescence measurement using pyrene as a probe (Lee et al., 2009). Briefly, pyrene dissolved in acetone was added to 10-mL empty volumetric flasks. After fully evaporating the acetone, 10 mL of HA-C_{18} and FA-HA-C_{18} solution with different concentrations ranging from 1.0×10^{-4} to 5×10^{-1} mg/mL were added into pyrene. The final concentration of pyrene was controlled at 6.0×10^{-7} M. The solutions were sonicated for 30 min in water bath and then kept at room temperature overnight to allow the solubilization equilibrium of pyrene. The fluorescence spectra of solutions were recorded on a fluorometer (F-2500, Hitachi Co., Japan). Excitation was carried out at 336 nm and emission spectrum was recorded from 360 nm to 450 nm. The intensity ratio of the first peak (I_1, 373 nm) to the third peak (I_3, 384 nm) was analyzed for the calculation of CMC.

2.5. Preparation of HA-C_{18} and FA-HA-C_{18} polymeric micelles

PTX-loaded polymeric micelles were prepared by probe-type ultrasonication technique (Du et al., 2009; Park et al., 2004). HA-C_{18} or FA-HA-C_{18} polymer (10 mg) was dispersed in distilled water to give a concentration of 1 mg/mL. PTX (10–30% amount of polymers) was dissolved in anhydrous ethanol, and then the PTX solution was

injected into polymer solution slowly with stirring at room temperature. The mixture was ultrasonicated for 10 min (active every 2 s for a 3 s duration with an output power of 200 W, JY92-II, Ningbo Xinzhi Scientific Instrument Institute, Zhejiang, China) in ice bath after stirred at room temperature for 24 h. The resultant PTX-loaded micellar solution was centrifuged at 3500 rpm for 20 min, and then filtered by 0.45 μm microfiltration membrane.

2.6. Characterizations of HA-C_{18} and FA-HA-C_{18} polymeric micelles

2.6.1. Particle size and zeta potential measurement

The average particle size and size distribution of the micelles were measured by dynamic light scattering instrument (Nicomp-380/ZLS, USA). The zeta potential was determined by using a zeta potential analyzer (Delsa 440 SX, Beckmann, USA).

2.6.2. Measurement of PTX concentration in micellar solution

The concentration of PTX in the micellar solution was determined by HPLC (LC-10ATvp, Shimadzu Corporation). The mobile phase consisted of acetonitrile and water (55:45, v/v). A phenomenex C_{18} column (250 mm × 4.6 mm, 5 μm) was used. The flow rate was 1.0 mL/min, the detection wavelength was 227 nm (UV detector, SPD-10Avp, Shimadzu Corporation), the column temperature was 35 °C and the injected volume of the sample was 20 μL.

2.6.3. Determination of drug encapsulation efficiency (EE) and drug loading (DL)

PTX-loaded micellar solution (200 μL) was diluted with 9.8 mL of methanol, followed by ultrasonic treatment in water bath at room temperature for 20 min. After being filtered with 0.22 μm microfiltration membrane, the PTX content was determined by HPLC method. The drug EE was calculated as the ratio of the drug amount in the micelles to the total drug amount added in the solution. And the DL was assayed as the percentage of the drug amount incorporated in the micelles of the total amount of the micelles.

2.6.4. Transmission electron microscopy (TEM) of PTX-loaded HA-C_{18} and FA-HA-C_{18} micelles

The morphology of the micelles was characterized using TEM (H-600, Hitachi, Japan). Before visualization, diluted dispersions of micelles were negatively stained with 1% phosphotungstic acid and finally examined through TEM.

2.6.5. Differential scanning calorimetry (DSC) measurement

DSC experiments were performed using TA-60 WS DSC-60 differential scanning calorimetry (Shimadzu, Japan) to study the physical properties of PTX, blank HA-C_{18} (FA-HA-C_{18}) micelles, physical mixture of PTX and blank HA-C_{18} (FA-HA-C_{18}) micelles, and PTX-loaded HA-C_{18} (FA-HA-C_{18}) micelles. The temperature ranged from 20 °C to 300 °C and the heating rate was 10 °C/min.

2.6.6. In vitro release of PTX from micelles

Release of PTX from PTX-loaded micelles was measured using a dialysis bag (molecular weight cutoff (MWCO) = 7000). Phosphate-buffered saline (PBS, 100 mL) at pH 7.4 containing 10% PEG 400, was employed as release medium. The PBS system was stirred with a speed of 100 rpm at 37 °C. PTX-loaded micelles containing 200 μg of PTX were placed in a dialysis bag and immersed in the medium. At predetermined time intervals, 5 mL aliquots of the medium was withdrawn and the same volume of fresh medium was added. The in vitro release behavior of the PTX-loaded micelles was measured by HPLC and compared with that of a commercial Taxol formulation. All assays were performed in triple.

2.7. In vitro cytotoxicity assays

MCF-7 cells, breast cancer cells, are of folate receptor (FR) overexpression. A549 cells, nonsmall-cell lung cancer (Alveolar type 2) cell lines, are FR deficient cell line. The two type cells were cultured in DMEM and RPMI 1640 culture medium respectively, containing 10% (v/v) fetal bovine serum and 100 IU/mL penicillin and 100 g/mL streptomycin at 37 °C in a humidified 5% CO_2–95% air atmosphere.

A comparison of in vitro cytotoxicity of Taxol and PTX-loaded micelles was performed on MCF-7 and A549 cells with an in vitro proliferation method using MTT. The cytotoxicity of blank micelles, and vehicle of Taxol (Cremophor EL:ethanol, 50:50 (v/v), further abbreviated as Taxol vehicle) were evaluated for comparison. Briefly, MCF-7 and A549 cells were seeded in 96-well plates at the density of 3×10^4 viable cells per well and incubated 24 h to allow cell attachment. The cells were then incubated with Taxol, PTX-loaded micelles (final concentrations of PTX were 1, 10, 100 ng/mL and 1, 10, 100 μg/mL), Taxol vehicle and blank micelles at 37 °C for 48 h. At determined time, 50 μL of MTT solution (2 mg/mL) was added and incubated for another 3.5 h at 37 °C. MTT was aspirated off and 200 μL of DMSO was added to dissolve the formazan crystals. Absorbance was measured at 570 nm using a BioRed microplate reader (Model 500, USA). Untreated cells were taken as control with 100% viability and cells without addition of MTT were used as blank to calibrate the spectrophotometer to zero absorbance. The relative cell viability (%) was calculated as (OD of treated cells/OD of nontreated cells) × 100.

2.8. In vitro cellular uptake

Cells were seeded in a 24-well plate at a seeding density of 1×10^5 cells per well and incubated 24 h to allow cell attachment. Then cells were incubated with Taxol, PTX-loaded micelles with PTX concentrations of 1 μg/mL for 2 h. After incubation, the medium was aspirated, the cells were washed with ice cold PBS (pH 7.4) thrice. The cells were scraped into a tube by adding 300 μL of distilled water. The collected cells were then subjected to probe-type ultrasonic treatment (active every 2 s for a 3 s duration with an output power of 200 W, 5 cycles) in ice bath. The PTX content in the cell lysate was analyzed by UPLC–MS/MS, and the cellular uptakes of PTX-loaded micelles were corrected to per microgram protein determined by Coomassie Brilliant Blue assay using a bovine serum albumin as standard.

2.9. Observation of internalization of drug loaded micelles

For investigation the intracellular localization of the PTX-loaded micelles, the fluorescent HA-C_{18} and FA-HA-C_{18} micelles were fabricated in a same way except loading with coumarin-6. MCF-7 cells were seeded onto coverglasses in a 6-well plate at a density of 2×10^5 cells per well and incubated 24 h to allow cell attachment. The free coumarin-6, coumarin-6-loaded HA-C_{18} and FA-HA-C_{18} micelles dispersed in the serum-free cell culture medium (the coumarin-6 concentration was 10 μg/mL) were added into the wells. Cells were washed three times by PBS after incubation for 0.5 and 2 h and then fixed by 70% ethanol for 20 min. The cells were further washed thrice with PBS and the nuclei were then counterstained with PI for 25 min. The fixed cell monolayer was finally washed thrice with PBS. The cover glasses were placed onto glass microscope slides and visualized using a confocal laser scanning microscope (CLSM, TCS SP2/AOBS, LEICA, Germany) equipped with Argon (488 nm) and He Ne (543 nm) lasers for fluorescence.

2.10. Folate and HA receptors competitive inhibition studies

In order to investigate the folate and CD44 dual receptors-mediated uptake of coumarin-6-loaded HA-C_{18} and FA-HA-C_{18}

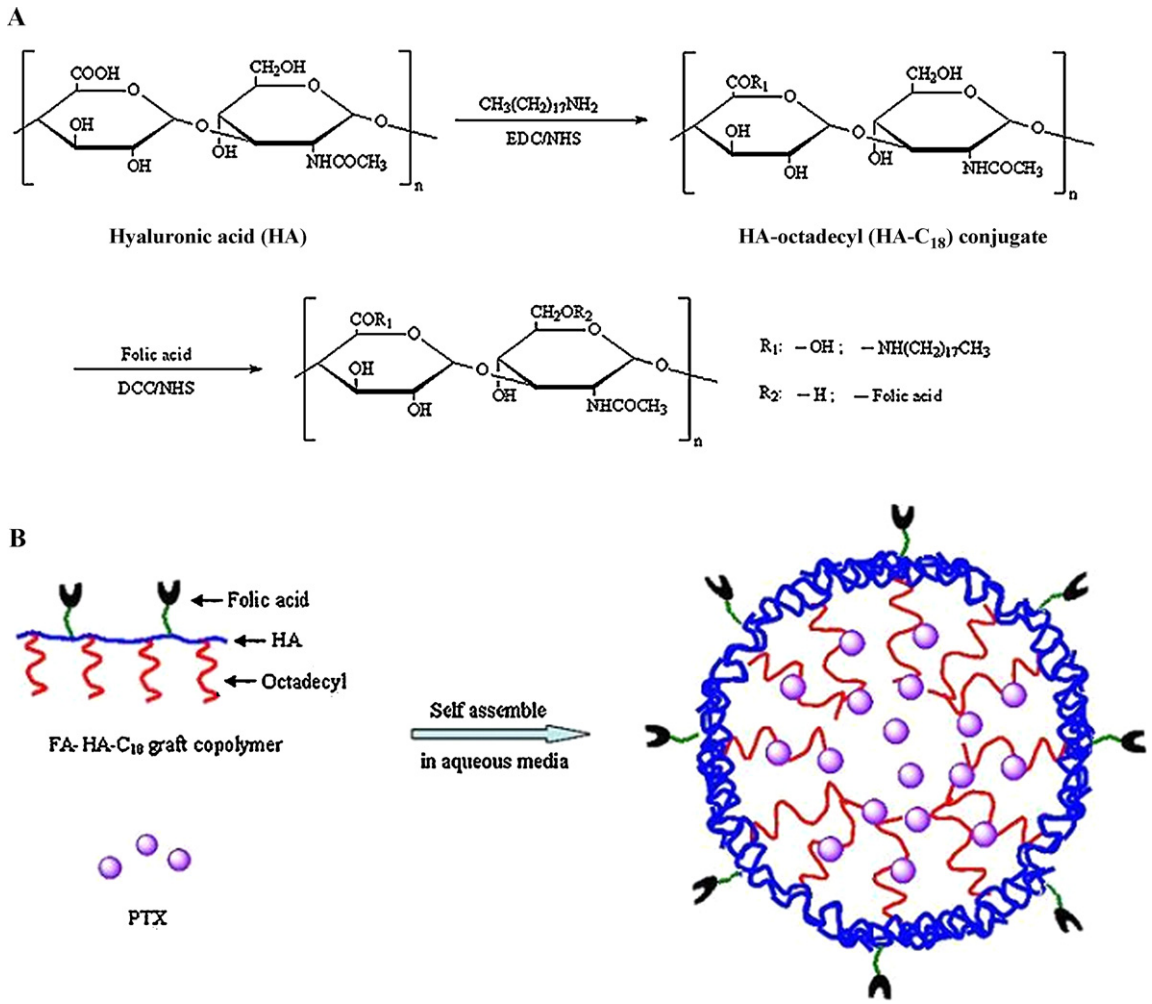

Fig. 1. Schematic representations for (A) synthesis of HA-C_{18} and FA-HA-C_{18} conjugates and (B) the self-assembled and drug-loading mechanisms of polymeric micelles from FA-HA-C_{18} graft copolymer in aqueous solution.

micelles, the culture medium was replaced with 2 mL of serum-free culture medium containing HA polymer (10 mg/mL) or free folic acid (1 mM) and coumarin-6-loaded HA-C_{18} and FA-HA-C_{18} micelles in MCF-7 and A549 cells (Xin et al., 2010). Followed by incubation for 2 h, the cells were then washed triplicate with PBS, then the intracellular localization of HA-C_{18} and FA-HA-C_{18} micelles were observed using fluorescence microscopy (Leica DM 1000, Leica Microsystems, Germany).

2.11. Exploring uptake pathways of HA-C_{18} and FA-HA-C_{18} micelles using endocytic inhibitors

The effects of several membrane entry inhibitors on PTX-loaded HA-C_{18} and FA-HA-C_{18} micelles' uptake were investigated by first incubating the MCF-7 cells for 1 h at 37 °C with a series of endocytic inhibitors, such as chlorpromazine (CPZ, 10 μg/mL), sucrose (0.45 M), indometacin (100 μM), colchicine (10 μM) and sodium azide (25 μM). Additionally, 1 mM free folic acid to inhibit the FR-mediated endocytosis only treating to PTX-loaded FA-HA-C_{18} micelles, and then treating the cells with PTX-loaded HA-C_{18} and FA-HA-C_{18} micelles (PTX concentration 1 μg/mL) for an additional 2 h. The following steps were processed as described in Section 2.8.

2.12. Statistical analysis

Two-sided, unpaired Student's *t*-test was applied to test the significance of differences between cellular uptake extent of Taxol, PTX-loaded HA-C_{18} and FA-HA-C_{18} micelles. The differences were considered to be significant at $P < 0.05$ and very significant at $P < 0.01$. All values were expressed as the mean value ± standard deviation (mean ± SD, $n = 3$ for cellular uptake).

3. Results and discussion

3.1. Synthesis and characterization of HA-C_{18} and FA-HA-C_{18} conjugates

The chemical conjugate of HA-C_{18} was synthesized by grafting the carboxyl group of HA with an amine group of octadecylamine in the presence of EDC and NHS. For FA-HA-C_{18} conjugate synthesis, folic acid was firstly activated by DCC/NHS and then conjugated onto HA backbone through the ester linker. The synthetic scheme is shown in Fig. 1A.

The chemical structure of HA, HA-C_{18}, FA-HA-C_{18} and DS of octadecyl on the backbone of HA was determined by ^{1}H NMR analysis. Fig. S1 (Supporting information) shows the ^{1}H NMR spectra of HA, HA-C_{18} and FA-HA-C_{18}. As shown in ^{1}H NMR spectrum of HA, N-acetyl (–$NHCOCH_3$) peak can be identified at δ (ppm) 1.95 along with glucosidic H (10H) at δ (ppm) 3.0–4.0 and anomeric H (2H) at δ (ppm) 4.35 and 4.45. Compared with HA, the ^{1}H NMR spectrum of HA-C_{18} showed new-emerged peaks at δ (ppm) 0.83 and 1.23, belonging to signals of the methyl (–CH_3) and the methylenes (–CH_2–) of the long-chain octadecyl group, respectively. The results

Table 1
The physicochemical characterization of HA-C_{18} (FA-HA-C_{18}) self-assembled micelles (mean ± SD, $n = 3$).

Samples[a]	Feed ratio[b]	DS (%)	CMC (μg/mL)	Size (nm)	PI	Zeta potential (mV)
HA-C_{18}-1	2/1	12.7	37.3	456.4 ± 13.9	0.350 ± 0.071	−37.9 ± 2.3
HA-C_{18}-2	1/1	16.2	18.9	330.2 ± 7.8	0.311 ± 0.057	−33.5 ± 1.5
HA-C_{18}-3	3/2	19.3	10.0	175.8 ± 4.8	0.261 ± 0.013	−30.1 ± 3.1
FA-HA-C_{18}	3/2 (20/1[c])	19.3 (6.8[d])	11.2	191.9 ± 8.7	0.242 ± 0.021	−33.0 ± 2.2

[a] HA-C_{18} conjugates with different DS values of octadecyl group.
[b] Molar feed ratio of octadecylamine to –COOH of HA polymer.
[c] Molar feed ratio of folic acid to –CH_2OH of HA polymer.
[d] DS of folic acid in FA-HA-C_{18} conjugate.

confirmed the successful conjugation of octadecyl group onto HA backbone. The grafting of folic acid to HA-C_{18} conjugate was confirmed by the appearance of weak signals at δ (ppm) 6.6–8.6, which corresponded to the aromatic protons of folic acid.

The DS, defined as the number of octadecyl group per 100 sugar residues of HA polymer, was controlled by varying the feed ratio of octadecylamine to –COOH of HA polymer. By calculating the relative intensity ratio of N-acetyl (–$NHCOCH_3$) peak in HA to methyl (–CH_3) peak in octadecyl group in ^{1}H NMR spectrum of HA-C_{18}, the DS of octadecyl to HA could be determined (Lee et al., 2009). The characteristics of HA-C_{18} (FA-HA-C_{18}) conjugates are summarized in Table 1. As expected, the DS of octadecyl increased as the feed ratio of octadecylamine increased. The DS of folic acid in FA-HA-C_{18} determined by UV method was 6.8%.

The CMC is an important parameter affecting the aggregation behavior of polymeric micelles in solution, that is, the self-assembled ability of the amphiphilic copolymer and the structural stability of micelles in vitro and in vivo. CMC values of HA-C_{18} with different DS of octadecyl and FA-HA-C_{18} in aqueous solution were studied by fluorescence spectroscopy using pyrene as a hydrophobic fluorescence probe. Fig. S2 (Supporting information) shows the change in the value of I_{373}/I_{384} against the logarithm of HA-C_{18} or FA-HA-C_{18} concentration. Compared with the traditional low-molecular-weight surfactants, HA-C_{18} and FA-HA-C_{18} polymers had a lower CMC value from 10.0 to 37.3 μg/mL, therefore possessed better in vitro and vivo structural integrity. That is, the HA-C_{18} and FA-HA-C_{18} micelles could remain stable in solution even under extreme dilution and preserve structural integrity after intravenous administration into the systemic circulation.

The CMC values of HA-C_{18} micelles with 12.7%, 16.2% and 19.3% DS of octadecyl in distilled water were determined to be 37.3, 18.9 and 10.0 μg/mL, respectively. It was easily observed that the CMC of the HA-C_{18} nanoaggregates decreased as the DS of the hydrophobic groups increased, because higher hydrophobicity makes the formed micelles more compact, and then results in the lower CMC. The CMC value of FA-HA-C_{18} micelle was 11.2 μg/mL, similar to that of HA-C_{18} micelle with the same DS (19.3%), indicating folate conjugation has little bearing on the micelle self-aggregation behavior. The similar findings were also found in the reported references (Du et al., 2009; Xu et al., 2007).

3.2. Preparation and characteristics of PTX-loaded HA-C_{18} and FA-HA-C_{18} micelles

Self-assembled micelles of hydrophobized polysaccharides can be prepared by a variety of techniques, including ultrasound, dialysis and emulsification, depending on the swelling property and solubility of modified polysaccharides in water. In the present study, PTX was physically incorporated into HA-C_{18} and FA-HA-C_{18} micelles using ultrasonic method. The method is simple and does not require adding stabilizer, emulsifier and other agents. In aqueous solution, hydrophobic interactions between grafted octadecyl chains contributed to form self-assembled nanoaggregates with several transient cross-links connecting polymer chains, and hydrophilic backbone of HA served as the shell of polymeric micelles responsible for providing an effective steric protection layer. Fig. 1B illustrated the self-assembled and drug-loading mechanisms of polymeric micelles from FA-HA-C_{18} graft copolymer in aqueous solution. The average particle size, polydispersity index (PI) and zeta potentials of HA-C_{18} and FA-HA-C_{18} blank micelles and EE, DL of PTX-loaded micelles are listed in Tables 1 and 2, respectively. The average sizes of blank HA-C_{18} micelles with different DS of octadecyl group were in the range of 175.8–456.4 nm. The results apparently indicated that the DS values significantly affected the size of HA-C_{18} micelles. The aggregation behavior, particle size and zeta potential of these micelles and drug loading extent can be controlled effectively by tuning the configuration of hydrophobized polysaccharides, length and number of branch chains, and modification sites of polysaccharides. The particle size decreased with the increase in the DS of octadecyl group, probably due to stronger hydrophobic strength and more compact micellar core packing. The size of PTX-loaded micelles with different drug loading amounts was in the range of 184.8–379.7 nm. For copolymers of HA-C_{18}-1 and HA-C_{18}-2, the sizes of PTX-loaded micelles were smaller than their corresponding blank micelles, suggesting the addition of hydrophobic PTX might induce the micellar core more compact. By contrast, the particle size of PTX-loaded micelles

Table 2
The physicochemical characterization of PTX-loaded HA-C_{18} (FA-HA-C_{18}) self-assembled micelles (mean ± SD, $n = 3$).

Sample	Drug/carrier (w/w, %)	Size (nm)	Zeta potential (mV)	EE (%)	DL (%)
HA-C_{18}-1	10	379.7 ± 4.4	−32.7 ± 0.9	89.0 ± 3.4	8.3 ± 0.2
	20	354.1 ± 7.6	−27.3 ± 1.7	82.6 ± 2.9	14.0 ± 0.4
	30	340.4 ± 2.5	−25.2 ± 3.9	74.4 ± 3.4	17.2 ± 0.8
HA-C_{18}-2	10	323.0 ± 7.1	−29.9 ± 4.2	91.9 ± 2.1	8.7 ± 0.2
	20	300.0 ± 7.2	−24.3 ± 3.0	86.9 ± 1.9	14.8 ± 0.3
	30	275.4 ± 8.1	−17.8 ± 1.9	77.8 ± 2.6	18.1 ± 0.8
HA-C_{18}-3	10	184.8 ± 6.4	−25.7 ± 2.2	97.0 ± 3.6	8.8 ± 0.1
	20	196.0 ± 5.6	−21.5 ± 3.2	90.6 ± 3.3	15.5 ± 0.1
	30	206.9 ± 2.7	−19.9 ± 2.0	82.6 ± 8.0	18.8 ± 1.4
FA-HA-C_{18}	10	206.1 ± 14.2	−27.3 ± 1.9	97.3 ± 4.1	8.9 ± 0.2
	20	218.3 ± 6.4	−23.9 ± 0.6	89.7 ± 1.1	15.5 ± 0.8
	30	230.5 ± 8.5	−19.4 ± 1.3	81.0 ± 2.8	18.8 ± 0.7

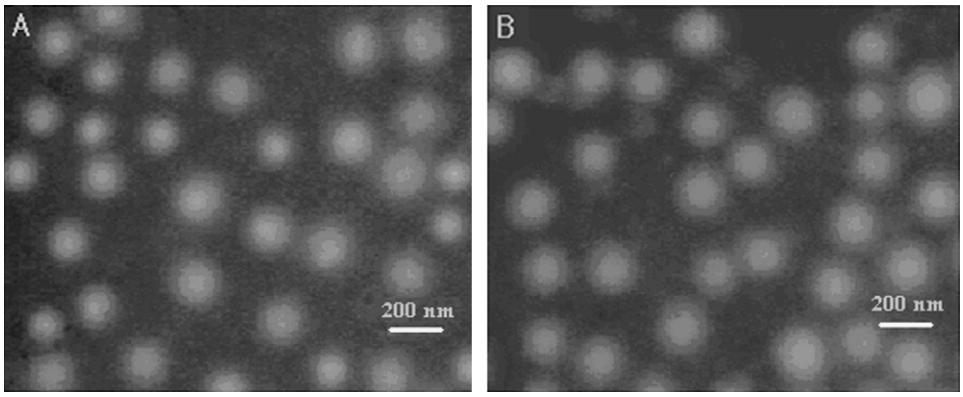

Fig. 2. Transmission electron micrographs of PTX-loaded HA-C_{18}-3 micelles (A) and FA-HA-C_{18} micelles (B).

was larger than those of blank micelles for copolymers of HA-C_{18}-3 and FA-HA-C_{18}. It could be explained that the HA-C_{18} (FA-HA-C_{18}) with highest DS formed micelles with so tightly packed hydrophobic core that the drug loading results in the increase of the micellar core volume.

The zeta potentials of blank and PTX-loaded micelles were negative and ranged from −17.8 to −37.9 mV (Tables 1 and 2), indicating that the micellar surface was covered by the negatively charged HA polymers. The increase of DS also reduced the carboxyl groups of HA-C_{18}, and further resulted in a decrease of the surface charge of blank micelles. The negative charge surface of HA micelles could provide a physical stability for PTX-loaded micelles in aqueous solution.

EE and DL capacities are two critical parameters for evaluating the capacity of a selected polymer to entrap the drug. The EE and DL values of PTX in HA-C_{18} (FA-HA-C_{18}) micelles are summarized in Table 2. The DL capacity enhanced with the increase in the DS of octadecyl group in PTX-loaded HA-C_{18} micelles. These results could be explained by the fact that the higher the DS of octadecyl group in HA-C_{18}, the stronger the binding affinity between hydrophobic PTX and the hydrophobic micellar core region.

Formation of PTX-loaded HA-C_{18}-3 and FA-HA-C_{18} micelles was also examined using TEM. Transmission electron micrographs of PTX-loaded HA-C_{18} and FA-HA-C_{18} micelles are presented in Fig. 2, showing spherical micellar nanoparticle with uniform size.

To confirm the existence form of PTX in the polymeric micelles, DSC analysis was carried out for PTX, blank micelles, the physical mixture of PTX and blank micelles and PTX-loaded micelles. As shown in Fig. S3 (Supporting information), calorimetric curves of PTX exhibited an endothermic peak at 227 °C and an exothermic peak at 240 °C. The former was the melting point of PTX and the latter was considered to be the degradation point. The blank micelles of HA-C_{18}-3 (FA-HA-C_{18}) showed no endothermic peak. The physical mixtures of them showed all characteristic peaks of each component only with slightly shift. The PTX-loaded HA-C_{18}-3 (FA-HA-C_{18}) micelles exhibited a similar calorimetric curve to the blank micelles, and no obvious melting peak of PTX appeared, suggesting that PTX was converted from the crystalline state to the amorphous state after loading into polymeric micelles.

In vitro release behavior of Taxol, PTX-loaded HA-C_{18} and FA-HA-C_{18} micelles was carried out in PBS (pH 7.4) containing 10% PEG 400 at 37 °C. As shown in Fig. 3, Taxol released 92.4% of PTX in 16 h. However, the HA-C_{18}-1, HA-C_{18}-2, HA-C_{18}-3 and FA-HA-C_{18} micelles released 71.3%, 61.6%, 52.8% and 55.2% of PTX at 192 h, respectively. It was obviously indicated that the release of PTX from the polymeric micelles was in a near zero-order sustained manner, and the hydrophobic core of micelles strongly restricted the migration of PTX into the release medium. The results also suggested the PTX release from the PTX-loaded HA-C_{18} micelles was delayed with the increasing DS of octadecyl group, caused by the enhanced hydrophobic interaction between PTX and hydrophobic core region.

3.3. In vitro cytotoxicity assays

The cell viability of blank micelles and PTX-loaded micelles against MCF-7 and A549 cells were evaluated, as compared with Taxol blank vehicle Cremophor EL and Taxol. As shown in Fig. S4 (Supporting information), blank micelles did not show any toxicity even at the highest concentration, while a strong cytotoxicity was observed when the cells were incubated in the presence of a high concentration of Cremophor EL. Therefore, it could be expected that HA-C_{18} and FA-HA-C_{18} blank micelles are far less toxic than Cremophor EL. As shown in Fig. 4, compared to micelles, Taxol showed a slightly stronger cytotoxicity at a concentration of 10 and 100 μg/mL, partially due to the toxicity of Cremophor EL vehicle. However, PTX-loaded HA-C_{18} and FA-HA-C_{18} micelles exhibited much higher cytotoxicity than Taxol even in a low PTX concentration below 0.1 μg/mL. It was reported previously that both MCF-7 and A549 cells were CD44 receptor overexpressing cell lines (Lee et al., 2008; Taetz et al., 2009). Compared to passive diffusion of free PTX through the cell membrane, the higher cytotoxicity of HA-C_{18} (FA-HA-C_{18}) micelles might be attributed to the higher binding affinity of HA derivatives to CD44 receptor. As a result, more PTX could be easily taken up by cells via a CD44 receptor-mediated

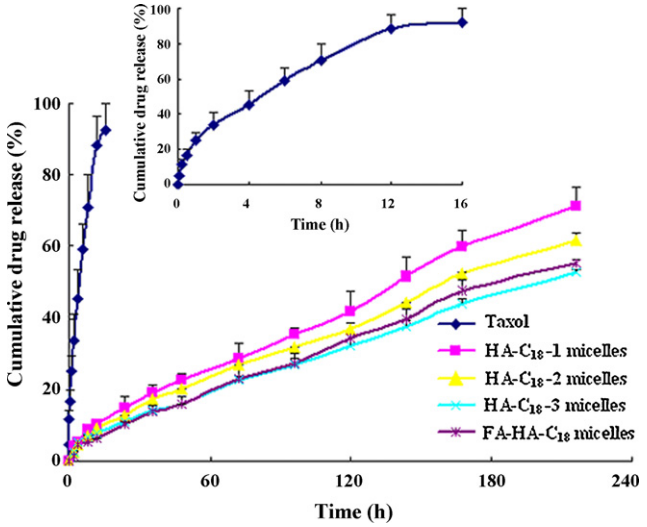

Fig. 3. In vitro drug release profiles of Taxol, PTX-loaded HA-C_{18} and FA-HA-C_{18} (30% of PTX adding amount) micelles. Data represented the mean ± SD (n = 3).

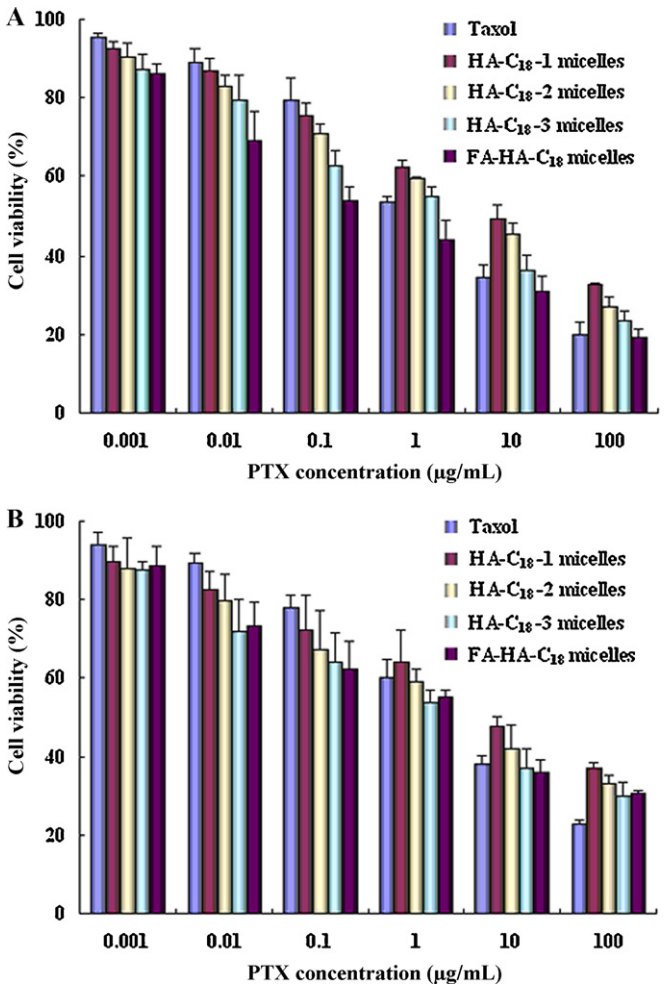

Fig. 4. In vitro cytotoxicity of Taxol, PTX-loaded HA-C_{18} and FA-HA-C_{18} micelles against (A) MCF-7 and (B) A549 cells (mean ± SD, $n = 3$).

endocytosis for polymeric micelles. Additionally, the cellular inhibition of FA-HA-C_{18} micelles was significantly greater than that by HA-C_{18}-3 micelles for FR-positive MCF-7 cells (Fig. 4A). On the other hand, FA-HA-C_{18} micelles showed a similar inhibitory effect to HA-C_{18}-3 micelles in FR-negative A549 cells (Fig. 4B). Accordingly, the enhanced cytotoxicity of FA-HA-C_{18} micelles, as compared with HA-C_{18}-3 micelles, could be explained by the enhanced cellular uptake via FR-mediated endocytosis in MCF-7 cells.

In addition, the enhanced cytotoxicity of HA-C_{18} micelles was observed as DS of octadecyl group increased from 12.7% to 19.3%, as shown in Fig. 4. It could be explained that the particle size of micelles decreased as the DS values increased as previously described. Therefore, micelles with higher DS value could be more efficiently taken up by cells via an endocytotic process, and delivered more PTX into cells for increased cytotoxicity.

3.4. In vitro cellular uptake studies

In order to investigate the effect of particle size and receptor-mediated endocytosis pathway on cellular uptake, the cellular accumulation of PTX in different formulations was compared in MCF-7 and A549 cells, respectively. As shown in Fig. 5, more PTX was taken up in the cells after PTX was encapsulated by the micelles, as compared with Taxol, which might be attributed to the endocytosis mediated by CD44 receptor. With increase in DS between 12.7% and 19.3%, cellular uptake amounts of PTX in

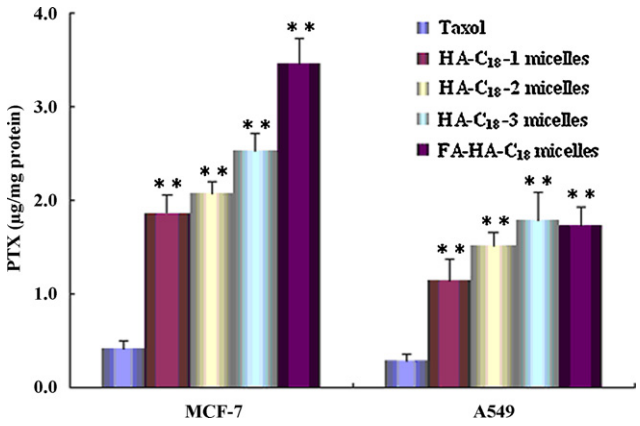

Fig. 5. Cellular uptake of PTX in MCF-7 and A549 cells after incubated with Taxol, PTX-loaded HA-C_{18} and FA-HA-C_{18} micelles at PTX concentration of 1 μg/mL for 2 h.

HA-C_{18} micelles were 4.5-, 5.0-, 6.2-fold, and 4.1-, 5.4-, 6.4-fold higher than that of Taxol in MCF-7 and A549 cells, respectively. The results demonstrated the particle size played a key role in the cellular uptake of HA-C_{18} micelles, and the smaller size of HA-C_{18} micelles might facilitate the transport across cell membrane and thus subsequent increase cellular uptake. Additionally, there was no significant difference between the intracellular uptake of HA-C_{18}-3 micelles and that of FA-HA-C_{18} micelles for A549 cells. However, compared with HA-C_{18}-3 micelles, the targeting effect of folic acid conjugation of FA-HA-C_{18} micelles was significant, with 36.7% uptake increase by MCF-7 cells. The in vitro cellular uptake mechanisms of HA-C_{18} micelles could be assumed to be the nonspecific and CD44-mediated endocytosis. As for FA-HA-C_{18} micelles, the FR-mediated endocytosis could further aid in the cellular uptake.

3.5. Observation of internalization of drug loaded micelles

To confirm the cellular uptake mechanism of HA-C_{18} and FA-HA-C_{18} micelles, coumarin-6 was employed as fluorescent probe using MCF-7 cells as the model cells. After the cells were incubated with free coumarin-6 solution, coumarin-6-loaded HA-C_{18}-3 and FA-HA-C_{18} micelles for different incubation times, the fluorescent intensity of coumarin-6 in cells was qualitatively observed by CLSM. As seen in Fig. 6, the images obtained from FITC channel showed the green fluorescence of the coumarin-6-loaded HA-C_{18}-3 and FA-HA-C_{18} micelles, and the images obtained from the PI channel showed the nuclei in red fluorescence stained by the PI. It could be seen in the merged channels of FITC and PI, the nuclei were surrounded closely by the coumarin-6-loaded micelles internalized into the cytoplasm in 0.5 h. The fluorescence intensity of coumarin-6-loaded in HA-C_{18}-3 and FA-HA-C_{18} micelles was obviously increased compared with the free coumarin-6 solution, due to non-specific and CD44-mediated endocytosis mechanisms of micelles. Furthermore, the stronger fluorescent signals were observed in FA-HA-C_{18} micelles compared to that of HA-C_{18}-3 micelles. It could be explained that folic acid conjugated micelles were able to be efficiently internalized into the cells via FR-mediated endocytosis, which promoted the entry of micelles into FR-overexpressed MCF-7 cells. After incubating 2 h, the fluorescence of HA-C_{18}-3 and FA-HA-C_{18} micelles was much brighter in the cytoplasm than those of 0.5 h, and the fluorescence became evenly dispersed in the nuclei. This meant that the cellular uptakes of free coumarin-6, coumarin-6-loaded HA-C_{18}-3 and FA-HA-C_{18} micelles were time-dependent.

The quantitative and qualitative cellular uptake experiments showed that the folate and CD44 receptors dual-targeting of

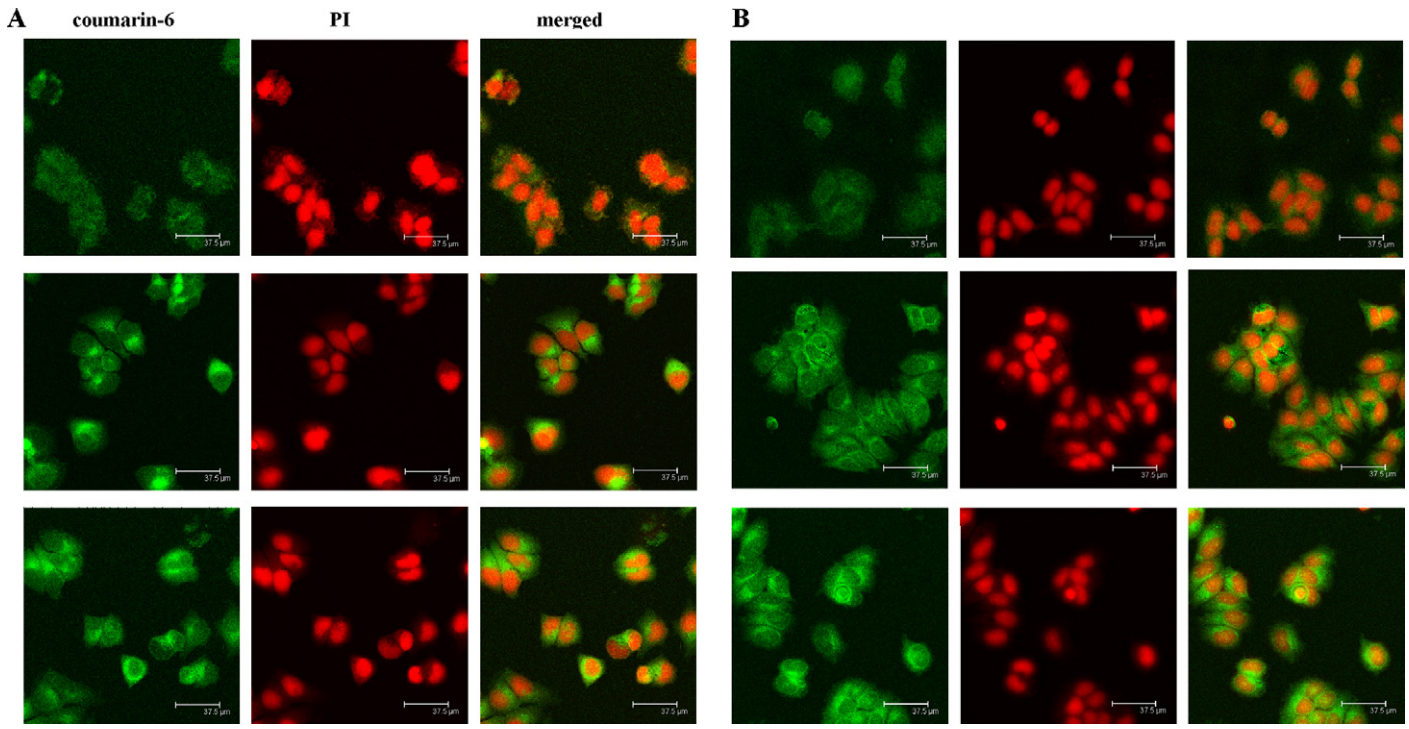

Fig. 6. CLSM of MCF-7 cells after 0.5 h (A) and 2 h (B) incubate with free coumarin-6 (up), coumarin-6-loaded HA-C_{18}-3 micelles (middle) and coumarin-6-loaded FA-HA-C_{18} micelles (bottom).

FA-HA-C_{18} micelles exhibited higher cellular uptake amount compared to the CD44 receptor single-targeting HA-C_{18} micelles. Fig. 7 illustrated the targeting performance and mechanism of CD44 receptor single-targeting HA-C_{18} micelles and folate and CD44 receptors dual-targeting FA-HA-C_{18} micelles. Compared with HA-C_{18} micelles only single binding to CD44 receptor, FA-HA-C_{18} could internalize more micelles into cells by concurrently interacting with folate and CD44 receptors on the surface of MCF-7 cells. Therefore, FA-HA-C_{18} micelles exhibited excellent cellular uptake performance via dual-receptor targeting strategy.

3.6. Folate and CD44 receptors competitive inhibition studies

To further confirm whether FA-HA-C_{18} micelles could be taken up by cells via CD44 and folate dual receptors-mediated endocytosis, a competitive inhibition experiment was performed by adding free HA polymer or free folic acid in the culture medium to block CD44 or folate receptors on cells. As shown in Fig. 8, the fluorescence intensity of coumarin-6-loaded HA-C_{18}-3 and FA-HA-C_{18} micelles was much stronger than those of micelles in the presence of free HA polymer for both MCF-7 and A549 cells. These results clearly supported the important role of CD44 receptor-mediated

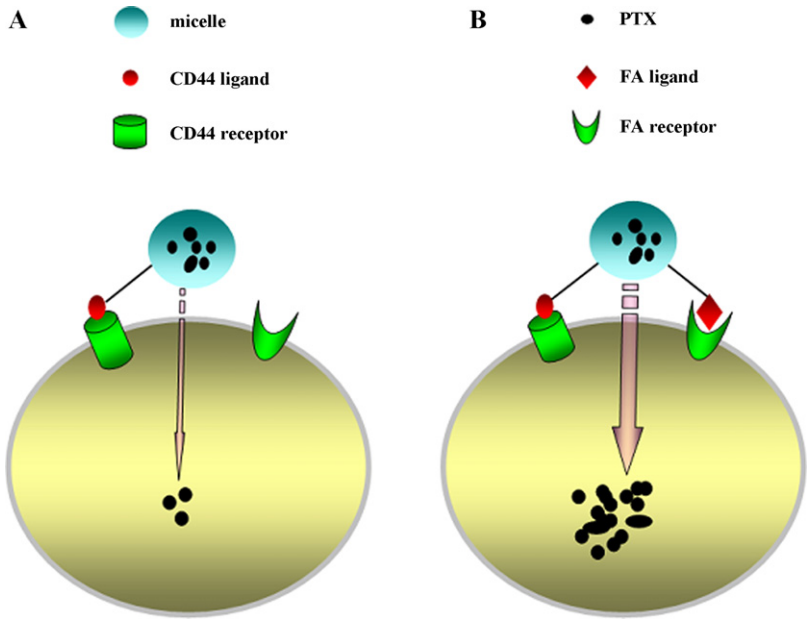

Fig. 7. Schematic illustration of targeting mechanism of HA-C_{18} micelles (A) and FA-HA-C_{18} micelles (B).

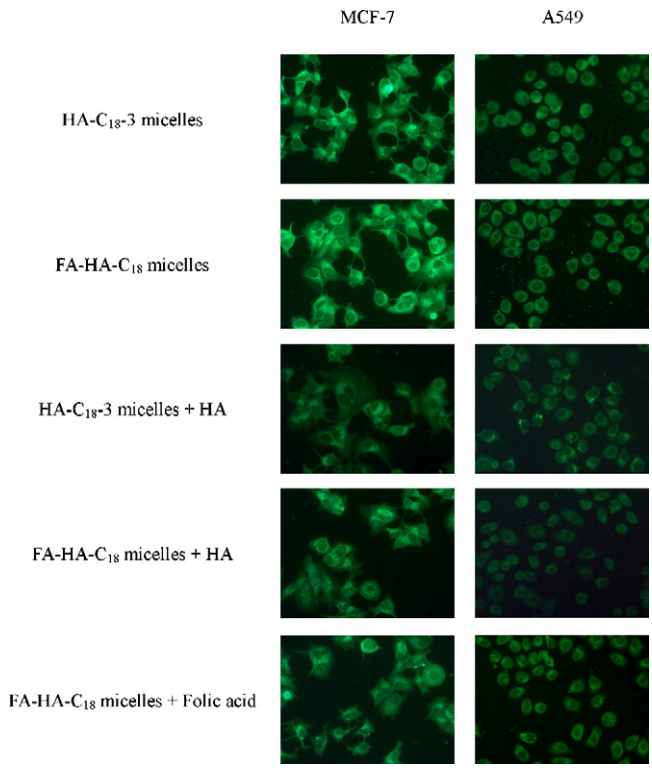

Fig. 8. Fluorescence microscopy images of coumarin-6 after cell uptake in MCF-7 and A549 cells incubated with coumarin-6-loaded HA-C_{18}-3 and FA-HA-C_{18} micelles for 2 h in the presence or absence of free HA or free folic acid.

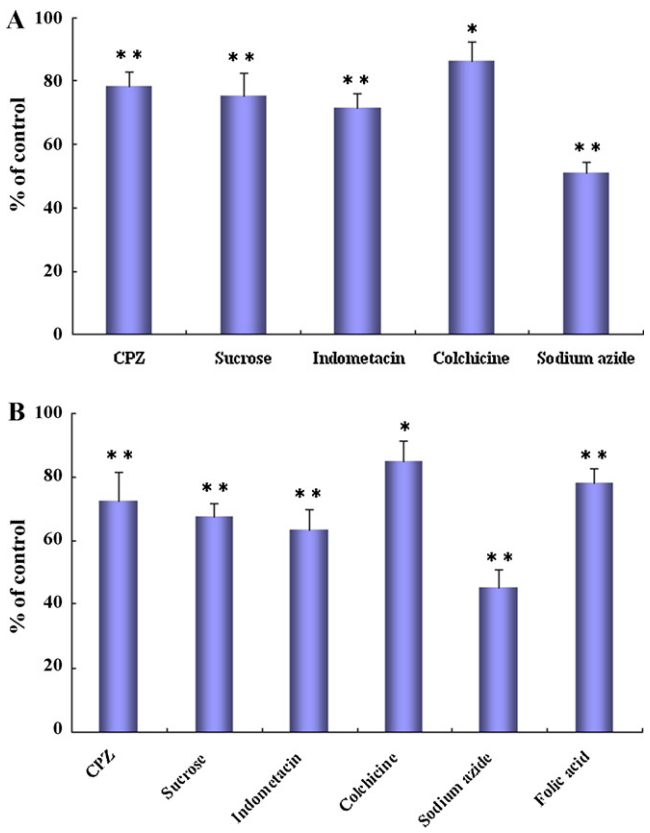

Fig. 9. Effects of added endocytic inhibitors on cellular uptake of PTX-loaded HA-C_{18}-3 (A) and FA-HA-C_{18} (B) micelles in MCF-7 cells.

endocytosis in efficient intracellular delivery of HA-C_{18}-3 and FA-HA-C_{18} micelles. For FR-overexpressed MCF-7, the fluorescence intensity of coumarin-6-loaded FA-HA-C_{18} micelles was exceedingly greater than that of coumarin-6-loaded HA-C_{18}-3 micelles in the folic acid-free medium. However, When 1 mM folic acid was added into the medium, the fluorescence intensity of coumarin-6-loaded FA-HA-C_{18} micelles was substantially reduced, with similar uptake amount to that of HA-C_{18}-3 micelles. In contrast, as for the FR-deficient cell line A549, the uptake amounts of coumarin-6-loaded HA-C_{18}-3, FA-HA-C_{18} and FA-HA-C_{18} in the presence of free folic acid in culture medium had no significant difference. Taken together, these results indicated the increased amount of coumarin-6-loaded FA-HA-C_{18} micelles internalized into MCF-7 cells was dependent on FR-mediated endocytosis.

3.7. *Exploring uptake pathways of PTX-loaded HA-C_{18} and FA-HA-C_{18} micelles*

In general, the intracellular fate of the macromolecular carriers is strongly affected by the route of entry. Endocytosis is a conserved process in eukaryotes where extracellular substances are taken up into the cells usually by the investigation of plasma membrane forming vesicles. Several endocytic pathways for macromolecules are identified to date: clathrin-mediated endocytosis, caveolae-mediated endocytosis, macropinocytosis, and clathrin- and caveolae-independent endocytosis (Nam et al., 2009). Clathrin-mediated endocytosis serves as the most prominent mechanism for the cellular entry. Caveolae are slowly internalized and small in size, and their fluid-phase volume is small. Thus, it is unlikely that they contribute significantly to constitutive endocytosis. Macropinocytosis refers to the formation of large endocytic vehicles, which is an efficient route for the nonselective endocytosis of nanoparticles with larger size.

In order to identify uptake mechanisms involved in the cellular entry of PTX-loaded HA-C_{18}-3 and FA-HA-C_{18} micelles, we employed several endocytic inhibitors, each known to be specific for a particular endocytic pathway. CPZ can dissociate the complex of clathrin and AP2 protein from the surface membrane of cells to inhibit the clathrin-mediated endocytosis (Wang et al., 1993). Hypertonic sucrose solution incubated with cells can inhibit endocytosis by leading to dissociate of the clathrin (Tahara et al., 2009). Indometacin is a specific inhibitor of caveolae-mediated endocytosis (Chang et al., 2009). Colchicine is a specific inhibitor of macropinocytosis by interfering with microtubule trafficking through binding to tubulin subunits. Sodium azide is an inhibitor of energy metabolism. It reduces the generation of intracellular ATP by inhibiting the cytochrome C oxidase of mitochondrial electron transport chain (Kim et al., 2006).

As shown in Fig. 9, CPZ, sucrose, indometacin, colchicine and sodium azide had significant effects on cellular uptake of PTX-loaded HA-C_{18}-3 and FA-HA-C_{18} micelles in MCF-7 cells. Additionally, 1 mM free folic acid could markedly inhibit the endocytosis of FA-HA-C_{18} micelles. The above results might suggested the endocytosis of PTX-loaded HA-C_{18}-3 and FA-HA-C_{18} micelles was energy-dependent, and the internalization of PTX-loaded HA-C_{18}-3 and FA-HA-C_{18} micelles was mediated by clathrin-mediated, caveolae-mediated endocytosis and macropinocytosis. The presence of free folic acid could inhibit the endocytosis of FA-HA-C_{18} micelles mediated by FR-mediated endocytosis. It was previously reported that FR-mediated endocytosis mechanisms were complex and along with clathrin- and caveolae-independent endocytosis it could also involve clathrin-mediated endocytosis (Sahay et al., 2010). In this study, our results of FA-HA-C_{18} micelles entry into MCF-7 cells coincided well with the above description, and the cellular uptake pathways involved multiple endocytosis pathways.

The cellular uptake of HA-C_{18}-3 and FA-HA-C_{18} micelles was completed by enclosing them into endosomes. The early endosomes matured into late endosomes or multivesicular bodies. These endosomes formed by clathrin-mediated endocytosis pathway were sorted to lysosomes later and to trans-Golgi network. Endosomes formed by caveolae-mediated endocytosis could be directly transport to the Golgi and/or endoplasmic reticulum, which could bypass lysosomes. Macropinocytosis usually accompanied by simply merging with the cell membrane or forming an intracellular vacuole, termed as a macropinosome.

4. Conclusion

A series of novel dual targeting micellar delivery systems based HA-C_{18} and FA-HA-C_{18} amphiphilic graft copolymers were developed for physical encapsulation with PTX. The newly developed nanomicellar systems had excellent performance features characterized by small particle size, high drug encapsulation efficiency and loading capacity, sustained-release characteristics, dual targeting ability and excellent cellular uptake into tumor cells. Therefore, the present study suggested that HA-C_{18} and FA-HA-C_{18} copolymers could be useful as biodegradable, biocompatible, and folate and CD44 receptors dual targeting nanostructure carriers for intercellular delivery of hydrophobic anticancer drugs, in particular for PTX.

Acknowledgements

We would like to acknowledge the support of this work by Key Project for Drug Innovation (2009ZX09301-012 and 2010ZX09401-304) and the National Basic Research Program of China (973 program, 2009CB930300).

Appendix A. Supplementary data

Supplementary data associated with this article can be found, in the online version, at doi:10.1016/j.ijpharm.2011.09.006.

References

Akiyoshi, K., Deguchi, S., Moriguchi, N., Yamaguchi, S., Sunamoto, J., 1993. Self-aggregates of hydrophobized polysaccharides in water. Formation and characteristics of nanoparticles. Macromolecules 26, 3062–3068.

Akiyoshi, K., Sunamoto, J., 1996. Supramolecular assembly of hydrophobized polysaccharides. Supramol. Sci. 3, 157–163.

Chang, J., Jallouli, Y., Kroubi, M., Yuan, X.B., Feng, W., Kang, C.S., Pu, P.Y., Betbeder, D., 2009. Characterization of endocytosis of transferrin-coated PLGA nanoparticles by the blood–brain barrier. Int. J. Pharm. 379, 285–292.

Choi, K.Y., Chung, H., Min, K.H., Yoon, H.Y., Kim, K., Park, J.H., Kwon, I.C., Jeong, S.Y., 2010. Self-assembled hyaluronic acid nanoparticles for active tumor targeting. Biomaterials 31, 106–114.

Choi, K.Y., Min, K.H., Na, J.H., Choi, K.W., Kim, K., Park, J.H., Kwon, I.C., Jeong, S.Y., 2009. Self-assembled hyaluronic acid nanoparticles as a potential drug carrier for cancer therapy: synthesis, characterization, and in vivo biodistribution. J. Mater. Chem. 19, 4102–4107.

Crosasso, P., Ceruti, M., Brusa, P., Arpicco, S., Dosio, F., Cattel, L., 2000. Preparation, characterization and properties of sterically stabilized paclitaxel-containing liposomes. J. Control. Release 63, 19–30.

Dosio, F., Reddy, L.H., Ferrero, A., Stella, B., Cattel, L., Couvreur, P., 2010. Novel nanoassemblies composed of squalenoyl-paclitaxel derivatives: synthesis, characterization and biological evaluation. Bioconjug. Chem. 21, 1349–1361.

Du, Y.Z., Wang, L., Yuan, H., Wei, X.H., Hu, F.Q., 2009. Preparation and characteristics of linoleic acid-grafted chitosan oligosaccharide micelles as a carrier for doxorubicin. Colloids Surf. B Biointerfaces 69, 257–263.

Fonseca, C., Simoes, S., Gaspar, R., 2002. Paclitaxel-loaded PLGA nanoparticles: preparation, physicochemical characterization and in vitro anti-tumoral activity. J. Control. Release 83, 273–286.

Grigorij, K., Ladislav, S., Robert, S., Peter, G., 2007. Hyaluronic acid: a natural biopolymer with a broad range of biomedical and industrial applications. Biotechnol. Lett. 29, 17–25.

Jaracz, S., Chen, J., Kuznetsova, L.V., Ojima, I., 2005. Recent advances in tumor-targeting anticancer drug conjugates. Bioorg. Med. Chem. 13, 5043–5054.

Jones, M.C., Leroux, J.C., 1999. Polymeric micelles – a new generation of colloidal drug carriers. Eur. J. Pharm. Biopharm. 48, 101–111.

Kan, P., Lin, X.Z., Hsieh, M.F., Chang, K.Y., 2005. Thermogelling emulsions for vascular embolization and sustained release of drugs. J. Biomed. Mater. Res. B Appl. Biomater. 75, 185–192.

Kim, J.S., Yoon, T.J., Yu, K.N., Noh, M.S., Woo, M., Kim, B.G., Lee, K.H., Sohn, B.H., Park, S.B., Lee, J.K., Cho, M.H., 2006. Cellular uptake of magnetic nanoparticle is mediated through energy-dependent endocytosis in A549 cells. J. Vet. Sci. 7, 321–326.

Larsen, N.E., Balazs, E.A., 1991. Drug delivery systems using hyaluronan and derivatives. Adv. Drug Deliv. Rev. 7, 279–293.

Lee, H., Ahn, C.H., Park, T.G., 2009. Poly[lactic-co-(glycolic acid)]-grafted hyaluronic acid copolymer micelle nanoparticles for target-specific delivery of doxorubicin. Macromol. Biosci. 9, 336–342.

Lee, H., Lee, K., Park, T.G., 2008. Hyaluronic acid–paclitaxel conjugate micelles: synthesis, characterization, and antitumor activity. Bioconjug. Chem. 19, 1319–1325.

Nam, H.Y., Kwon, S.M., Chung, H., Lee, S.Y., Kwon, S.H., Jeon, H., Kim, J., Kim, Y., Her, S., Oh, Y.K., Kwon, I.C., Kim, K., Jeong, S.Y., 2009. Cellular uptake mechanism and intracellular fate of hydrophobically modified glycol chitosan nanoparticles. J. Control. Release 135, 259–267.

Park, K., Kim, K., Kwon, I.C., Kim, S.K., Lee, S., Lee, D.Y., Byun, Y., 2004. Preparation and characterization of self-assembled nanoparticles of heparin–deoxycholic acid conjugates. Langmuir 20, 11726–11731.

Park, K., Lee, G.Y., Kim, Y.S., Yu, M., Park, R.W., Kim, I.S., Kim, S.Y., Byun, Y., 2006. Heparin–deoxycholic acid chemical conjugate as an anticancer drug carrier and its antitumor activity. J. Control. Release 114, 300–306.

Sahay, G., Alakhova, D.Y., Kabanov, A.V., 2010. Endocytosis of nanomedicines. J. Control. Release 145, 182–195.

Saul, J.M., Annapragada, A.V., Bellamkonda, R.V., 2006. A dual-ligand approach for enhancing targeting selectivity of therapeutic nanocarriers. J. Control. Release 114, 277–287.

Sharma, U.S., Balasubramanian, S.V., Straubinger, R.M., 1995. Pharmaceutical and physical properties of paclitaxel (Taxol) complexes with cyclodextrins. J. Pharm. Sci. 84, 1223–1230.

Taetz, S., Bochot, A., Surace, C., Arpicco, S., Renoir, J.M., Schaefer, U., Marsaud, V., Kerdine-Roemer, S., Lehr, C.M., Fattal, E., 2009. Hyaluronic acid-modified DOTAP/DOPE liposomes for the targeted delivery of anti-telomerase siRNA to CD44-expressing lung cancer cells. Oligonucleotides 19, 103–115.

Tahara, K., Sakai, T., Yamamoto, H., Takeuchi, H., Hirashima, N., Kawashima, Y., 2009. Improved cellular uptake of chitosan-modified PLGA nanospheres by A549 cells. Int. J. Pharm. 382, 198–204.

Torchilin, V.P., 2001. Structure and design of polymeric surfactant-based drug delivery systems. J. Control. Release 73, 137–172.

Wang, H.J., Zhao, P.Q., Liang, X.F., Gong, X.Q., Song, T., Niu, R.F., Chang, J., 2010. Folate-PEG coated cationic modified chitosan–cholesterol liposomes for tumor-targeted drug delivery. Biomaterials 31, 4129–4138.

Wang, L.H., Rothberg, K.G., Anderson, R.G., 1993. Mis-assembly of clathrin lattices on endosomes reveals a regulatory switch for coated pit formation. J. Cell Biol. 123, 1107–1117.

Wang, Y., Li, Y., Wang, Q., Wu, J., Fang, X., 2008. Pharmacokinetics and biodistribution of paclitaxel-loaded pluronic P105/L101 mixed polymeric micelles. Yakugaku Zasshi 128, 941–950.

Xin, D.C., Wang, Y., Xiang, J.N., 2010. The use of amino acid linkers in the conjugation of paclitaxel with hyaluronic acid as drug delivery system: synthesis, self-assembled property, drug release, and in vitro efficiency. Pharm. Res. 27, 380–389.

Xu, X.Y., Li, L., Zhou, J.P., Lu, S.Y., Yang, J., Yin, X.J., Ren, J.S., 2007. Preparation and characterization of N-succinyl-N′-octyl chitosan micelles as doxorubicin carriers for effective anti-tumor activity. Colloids Surf. B Biointerfaces 55, 222–228.

Ying, X., Wen, H., Lu, W.L., Du, J., Guo, J., Tian, W., Men, Y., Zhang, Y., Li, R.J., Yang, T.Y., Shang, D.W., Lou, J.N., Zhang, L.R., Zhang, Q., 2010. Dual-targeting daunorubicin liposomes improve the therapeutic efficacy of brain glioma in animals. J. Control. Release 141, 183–192.

Zhang, C., Qu, G.W., Sun, Y.J., Wu, X.L., Yao, Z., Guo, Q.L., Ding, Q.L., Yuan, S.T., Shen, Z.L., Ping, Q.N., Zhou, H.P., 2008. Pharmacokinetics, biodistribution, efficacy and safety of N-octyl-O-sulfate chitosan micelles loaded with paclitaxel. Biomaterials 29, 1233–1241.

Zheng, Y., Cai, Z., Song, X.R., Chen, Q.H., Bi, Y.Q., Li, Y.B., Hou, S.X., 2009. Preparation and characterization of folate conjugated N-trimethyl chitosan nanoparticles as protein carrier targeting folate receptor: in vitro studies. J. Drug Target. 17, 294–303.